

Testing realistic quark mass matrices in the custodial Randall-Sundrum model with flavor changing top decays

We-Fu Chang*

*Department of Physics, National Tsing Hua University, Hsin Chu 300, Taiwan*John N. Ng⁺ and Jackson M. S. Wu[‡]*Theory group, TRIUMF, 4004 Wesbrook Mall, Vancouver, British Columbia, Canada*

(Received 12 June 2008; published 4 November 2008)

We study quark mass matrices in the Randall-Sundrum (RS) model with bulk symmetry $SU(2)_L \times SU(2)_R \times U(1)_{B-L}$. The Yukawa couplings are assumed to be within an order of magnitude of each other, and perturbative. We find that quark mass matrices of the symmetrical form proposed by Koide *et al.* [Y. Koide, H. Nishiura, K. Matsuda, T. Kikuchi, and T. Fukuyama, Phys. Rev. D **66**, 093006 (2002)] can be accommodated in the RS framework with the assumption of hierarchyless Yukawa couplings, but not the Hermitian Fritzsch-type mass matrices. General asymmetrical mass matrices are also found which fit well simultaneously with the quark masses and the Cabibbo-Kobayashi-Maskawa matrix. Both left-handed (LH) and right-handed (RH) quark rotation matrices are obtained that allow analysis of flavor changing decay of both LH and RH top quarks. At a warped down scale of 1.65 TeV, the total branching ratio of $t \rightarrow Z + \text{jets}$ can be as high as $\sim 5 \times 10^{-6}$ for symmetrical mass matrices and $\sim 2 \times 10^{-5}$ for asymmetrical ones. This level of signal is within reach of the LHC.

DOI: 10.1103/PhysRevD.78.096003

PACS numbers: 11.30.Hv, 12.15.Ff, 13.85.-t, 14.65.Ha

I. INTRODUCTION

The idea of extra dimensions is by now a well-known one. It has led to new solutions to the gauge hierarchy problem without imposing supersymmetry [1,2], and it has opened up new avenues to attack the flavor puzzle in the standard model (SM). One such application is the seminal proposal of split fermions by Arkani-Hamed and Schmaltz [3] that fermion mass hierarchy can be generated from the wave function overlap of fermions located differently in the extra dimension. The split fermion scenario had been implemented in both flat extra dimension models [3,4], and warped extra dimension Randall-Sundrum (RS) models [5,6]. Subsequently, phenomenologically successful mass matrices were found in the case of one flat extra dimension without much fine-tuning of the Yukawa couplings [7], and in the case of warped extra dimensions, realistic fermion masses and mixing pattern can be reproduced with almost universal bulk Yukawa couplings [8–10].

To date, many attempts in understanding the fermion flavor structure come in terms of symmetries. Fermion mass matrix ansatz with a high degree of symmetry were constructed to fit simultaneously the observed mass hierarchy and flavor mixing patterns. It is an interesting question whether in the pure geometrical setting of the RS framework where there are no flavor symmetries *a priori*, such symmetrical forms can arise and arise naturally without fine-tuning of the Yukawa couplings, i.e. whether

symmetries in the fermion mass matrices can be compatible with a natural, hierarchyless Yukawa structure in the RS framework, and to what degree.

Another interesting and related question is whether or not one can experimentally discern if the fermion mass matrices are symmetric in the RS framework. In the SM, only the left-handed (LH) fermion mixings such as the Cabibbo-Kobayashi-Maskawa (CKM) mixing matrix is measurable, but not the right-handed (RH) ones. However, in the RS framework the RH fermion mixings become measurable through the effective couplings of the gauge bosons to the fermions induced from the Kaluza-Klein (KK) interactions. If the fermion mass matrices are symmetric, the LH and RH mixing matrices would be the same. Thus, the most direct way of searching for the effects of these RH mixings would be through the induced RH fermion couplings in flavor changing processes that are either not present or very much suppressed in the SM.

In this work we study how well the RS setting serves as a framework for flavor physics either with or without symmetries in the fermion mass matrices, and if the two scenarios can be distinguished experimentally. We concentrate on the quark (and especially the top) sector, and we study the issues involved in the RS1 model [2] with an $SU(2)_L \times SU(2)_R \times U(1)_X$ bulk symmetry, which we shall refer to as the minimal custodial RS (MCRS) model. The $U(1)_X$ is customarily identified with $U(1)_{B-L}$. The enlarged electroweak symmetry contains a custodial isospin symmetry which protects the SM ρ parameter from receiving excessive corrections, and the model has been shown to be a complete one that can pass all electroweak precision tests (EWPT) at a scale of ~ 3 to 4 TeV [11].

*wfchang@phys.nthu.edu.tw

+misery@triumf.ca

‡jwu@triumf.ca

The organization of the paper is as follows. In Sec. II we quickly review the details of the MCRS model to fix our notations. In Sec. III we investigate which type of mass matrix ansatz is compatible with Yukawa couplings that are perturbative and not fine-tuned by matching the ansatz form to that in the MCRS model. Relevant matching formulas and EWPT limits on the controlling parameters are collected into the two Appendices. We also investigate possible patterns in the mass matrices by numerically scanning the EWPT allowed parameter space for those that can reproduce simultaneously the observed quark masses and the CKM mixing matrix. In Sec. IV we study the effects of quark mass matrices being symmetrical or not are having on flavor changing top decays, $t \rightarrow c(u)Z$, which are expected to have the clearest signal at the LHC. We summarized our findings in Sec. V.

II. REVIEW OF THE MCRS MODEL

In this section, we briefly review the setup of the MCRS model. We summarize relevant results on the KK reduction and the interactions of the bulk gauge fields and fermions, and establish the notation to be used below.

A. General setup and gauge symmetry breaking

The MCRS model is formulated in a five-dimensional (5D) background geometry based on a slice of AdS_5 space of size πr_c , where r_c denotes the radius of the compactified fifth dimension. Two 3-branes are located at the boundaries of the AdS_5 slice, which are also the orbifold fixed points. They are taken to be $\phi = 0$ (UV) and $\phi = \pi$ (IR), respectively. The metric is given by

$$ds^2 = G_{AB} dx^A dx^B = e^{-2\sigma(\phi)} \eta_{\mu\nu} dx^\mu dx^\nu - r_c^2 d\phi^2, \quad (1)$$

where $\sigma(\phi) = kr_c|\phi|$, $\eta_{\mu\nu} = \text{diag}(1, -1, -1, -1)$, k is the AdS_5 curvature, and $-\pi \leq \phi \leq \pi$.

The model has $SU(2)_L \times SU(2)_R \times U(1)_X$ as its bulk gauge symmetry group. The fermions reside in the bulk, while the SM Higgs, which is now a bidoublet, is localized on the IR brane to avoid fine-tuning. The 5D action of the model is given by [11]

$$S = \int d^4x \int_0^\pi d\phi \sqrt{G} [\mathcal{L}_g + \mathcal{L}_f + \mathcal{L}_{\text{UV}} \delta(\phi) + \mathcal{L}_{\text{IR}} \delta(\phi - \pi)], \quad (2)$$

where \mathcal{L}_g and \mathcal{L}_f are the bulk Lagrangian for the gauge fields and fermions, respectively, and \mathcal{L}_{IR} contains both the Yukawa and Higgs interactions.

The gauge field Lagrangian is given by

$$\mathcal{L}_g = -\frac{1}{4} (W_{AB} W^{AB} + \tilde{W}_{AB} \tilde{W}^{AB} + \tilde{B}_{AB} \tilde{B}^{AB}), \quad (3)$$

where W , \tilde{W} , \tilde{B} are field strength tensors of $SU(2)_L$, $SU(2)_R$, and $U(1)_X$, respectively. On the IR brane, $SU(2)_L \times SU(2)_R$ is spontaneously broken down to $SU(2)_V$ when the SM Higgs acquires a vacuum expectation

value (VEV). On the UV brane, first the custodial $SU(2)_R$ is broken down to $U(1)_R$ by orbifold boundary conditions; this involves assigning orbifold parities under $S_1/(Z_2 \times Z_2')$ to the μ components of the gauge fields: one assigns $(-+)$ for $\tilde{W}_{\mu}^{1,2}$, and $(++)$ for all other gauge fields, where the first (second) entry refers to the parity on the UV (IR) boundary. Then, $U(1)_R \times U(1)_X$ is further broken down to $U(1)_Y$ spontaneously (via a VEV), leaving just $SU(2)_L \times U(1)_Y$ as the unbroken symmetry group.

B. Bulk gauge fields

Let $A_M(x, \phi)$ be a massless 5D bulk gauge field, $M = 0, 1, 2, 3, 5$. Working in the unitary gauge where $A_5 = 0$, the KK decomposition of $A_\mu(x, \phi)$ is given by (see e.g. [6,12])

$$A_\mu(x, \phi) = \frac{1}{\sqrt{r_c \pi}} \sum_n A_\mu^{(n)}(x) \chi_n(\phi), \quad (4)$$

where χ_n are functions of the general form

$$\chi_n = \frac{e^{\sigma}}{N_n} [J_1(z_n e^{\sigma}) + b_1(m_n) Y_1(z_n e^{\sigma})], \quad z_n = \frac{m_n}{k}, \quad (5)$$

that solve the eigenvalue equation

$$\left(\frac{1}{r_c^2} \partial_\phi e^{-2\sigma} \partial_\phi - m_n^2 \right) \chi_n = 0, \quad (6)$$

subject to the orthonormality condition

$$\frac{1}{\pi} \int_0^\pi d\phi \chi_n \chi_m = \delta_{mn}. \quad (7)$$

Depending on the boundary condition imposed on the gauge field, the coefficient function $b_1(m_n)$ is given by

$$(++) \text{ B.C.: } b_1(m_n) = -\frac{J_0(z_n e^{\sigma(\pi)})}{Y_0(z_n e^{\sigma(\pi)})} = -\frac{J_0(z_n)}{Y_0(z_n)}, \quad (8)$$

$$(-+) \text{ B.C.: } b_1(m_n) = -\frac{J_0(z_n e^{\sigma(\pi)})}{Y_0(z_n e^{\sigma(\pi)})} = -\frac{J_1(z_n)}{Y_1(z_n)}, \quad (9)$$

which in turn determine the gauge KK eigenmasses, m_n . For fields with the $(++)$ boundary condition, the lowest mode is a massless state $A_\mu^{(0)}$ with a flat profile

$$\chi_0 = 1, \quad (10)$$

while no zero mode exists if it is the $(-+)$ boundary condition. The SM gauge boson is identified with the zero mode of the appropriate bulk gauge field after KK reduction.

C. Bulk fermions

The free 5D bulk fermion action can be written as (see e.g. [5,6])

$$S_f = \int d^4x \int_0^\pi d\phi \sqrt{G} \left\{ E_a^M \left[\frac{i}{2} \bar{\Psi} \gamma^a (\tilde{\partial}_M - \tilde{\partial}_M) \Psi \right] + m \operatorname{sgn}(\phi) \bar{\Psi} \Psi \right\}, \quad (11)$$

where $\gamma^a = (\gamma^\mu, i\gamma^5)$ are the 5D Dirac gamma matrices in flat space, G is the metric given in Eq. (1), E_a^A the inverse vielbein, and $m = ck$ is the bulk Dirac mass parameter. There is no contribution from the spin connection because the metric is diagonal [5]. The form of the mass term is dictated by the requirement of Z_2 orbifold symmetry [5]. The KK expansion of the fermion field takes the form

$$\Psi_{L,R}(x, \phi) = \frac{e^{3\sigma/2}}{\sqrt{r_c \pi}} \sum_{n=0}^{\infty} \psi_{L,R}^{(n)}(x) f_{L,R}^n(\phi), \quad (12)$$

where the subscripts L and R label the chirality of the fields, and $f_{L,R}^n$ form two distinct sets of complete orthonormal functions, which are found to satisfy the equations

$$\begin{aligned} \left[\frac{1}{r_c} \partial_\phi - \left(\frac{1}{2} + c \right) k \right] f_R^n &= m_n e^\sigma f_L^n, \\ \left[-\frac{1}{r_c} \partial_\phi + \left(\frac{1}{2} - c \right) k \right] f_L^n &= m_n e^\sigma f_R^n, \end{aligned} \quad (13)$$

with the orthonormality condition given by

$$\frac{1}{\pi} \int_0^\pi d\phi f_{L,R}^{n*}(\phi) f_{L,R}^m(\phi) = \delta_{mn}. \quad (14)$$

Of particular interest are the zero modes which are to be identified as SM fermions:

$$f_{L,R}^0(\phi, c_{L,R}) = \sqrt{\frac{kr_c \pi (1 \mp 2c_{L,R})}{e^{kr_c \pi (1 \mp 2c_{L,R})} - 1}} e^{(1/2 \mp c_{L,R}) kr_c \phi}, \quad (15)$$

where the upper (lower) sign applies to the LH (RH) label. Depending on the Z_2 parity of the fermion, one of the chiralities is projected out. It can be seen that the LH zero mode is localized towards the UV (IR) brane if $c_L > 1/2$ ($c_L < 1/2$), while the RH zero mode is localized towards the UV (IR) brane when $c_R < -1/2$ ($c_R > -1/2$).

The higher fermion KK modes have the general form

$$\begin{aligned} f_{L,R}^n &= \frac{e^\sigma}{N_n} B_\alpha(z_n e^\sigma), \\ B_\alpha(z_n e^\sigma) &= J_\alpha(z_n e^\sigma) + b_\alpha(m_n) Y_\alpha(z_n e^\sigma), \end{aligned} \quad (16)$$

where $\alpha = |c \pm 1/2|$ with the LH (RH) mode takes the upper (lower) sign. Depending on the type of the boundary condition a fermion field has, the coefficient function $b_\alpha(m_n)$ takes the form [11]

$$(+ +) \text{ B.C.: } b_\alpha(m_n) = -\frac{J_{\alpha \mp 1}(z_n e^{\sigma(\pi)})}{Y_{\alpha \mp 1}(z_n e^{\sigma(\pi)})} = -\frac{J_{\alpha \mp 1}(z_n)}{Y_{\alpha \mp 1}(z_n)}, \quad (17)$$

$$(- +) \text{ B.C.: } b_\alpha(m_n) = -\frac{J_{\alpha \mp 1}(z_n e^{\sigma(\pi)})}{Y_{\alpha \mp 1}(z_n e^{\sigma(\pi)})} = -\frac{J_\alpha(z_n)}{Y_\alpha(z_n)}, \quad (18)$$

and normalization factor can be written as [11]

$$(+ +) \text{ B.C.: } N_n^2 = \frac{e^{2\sigma(\phi)}}{2kr_c \pi} B_\alpha^2(z_n e^{\sigma(\phi)}) \Big|_{\phi=0}^{\phi=\pi}, \quad (19)$$

$$(- +) \text{ B.C.: } N_n^2 = \frac{1}{2kr_c \pi} [e^{2\sigma(\pi)} B_\alpha^2(z_n e^{\sigma(\pi)}) - B_{\alpha \mp 1}^2(z_n)]. \quad (20)$$

The upper sign in the order of the Bessel functions above applies to the LH (RH) mode when $c_L > -1/2$ ($c_R < 1/2$), while the lower sign applies to the LH (RH) mode when $c_L < -1/2$ ($c_R > 1/2$). The spectrum of fermion KK masses is found from the coefficient function relations given by Eqs. (17) and (18).

Now there is an additional $SU(2)_R$ gauge symmetry over the SM in the bulk, and the fermions have to be embedded into its representations. Below we chose the simplest way of doing this, viz. the LH fermions are embedded as $SU(2)_R$ singlets, while the RH fermions are doublets [11]. Note that since the $SU(2)_R$ is broken on the UV brane by the orbifold boundary condition, one component of the doublet under it must be even under the Z_2 parity, and the other odd. This forces a doubling of RH doublets where the upper component, say the up-type quark, of one doublet, and the lower component of the other doublet, the down-type, are even.

D. Fermion interactions

In 5D, the interaction between fermions and a bulk gauge boson is given by

$$S_{f\bar{f}A} = g_5 \int d^4x d\phi \sqrt{G} E_a^M \bar{\Psi} \gamma^a A_M \Psi + \text{H.c.}, \quad (21)$$

where g_5 is the 5D gauge coupling constant. After KK reduction, couplings of the KK modes in the 4D effective theory arise from the overlap of the wave functions in the bulk. In particular, the coupling of the m th and n th fermion KK modes to the q th gauge KK mode is given by

$$g_{f\bar{f}A}^{mnq} = \frac{g_4}{\pi} \int_0^\pi d\phi f_{L,R}^m f_{L,R}^n \chi_q, \quad g_4 = \frac{g_5}{\sqrt{r_c \pi}}, \quad (22)$$

where $g_4 \equiv g_{\text{SM}}$ is the 4D SM gauge coupling constant. Note that since the gauge zero mode has a flat profile [Eq. (10)], by the orthonormality condition of the fermions wave functions, Eq. (14), only fermions of the same KK level couple to the gauge zero mode, and the 4D coupling is simply given by $g_{f\bar{f}A}^{mm0} = g_4$.

With the Higgs field Φ localized on the IR brane, the Yukawa interactions are contained entirely in \mathcal{L}_{IR} of the 5D action (2). The relevant action on the IR brane is given

by

$$S_{\text{Yuk}} = \int d^4x d\phi \sqrt{G} \delta(\phi - \pi) \times \frac{\lambda_{5,ij}}{kr_c} \bar{\Psi}_i(x, \phi) \Psi_j(x, \phi) \Phi(x) + \text{H.c.}, \quad (23)$$

where $\lambda_{5,ij}$ are the dimensionless 5D Yukawa coupling, and i, j the family indices. Rescaling the Higgs field to $H(x) = e^{-kr_c\pi} \Phi(x)$ so that it is canonically normalized, the effective 4D Yukawa interaction obtained after spontaneous symmetry breaking is given by

$$S_{\text{Yuk}} = \int d^4x v_W \frac{\lambda_{5,ij}}{kr_c \pi} \sum_{m,n} \bar{\psi}_{iL}^{(m)}(x) \psi_{jR}^{(n)}(x) f_L^m(\pi, c_i^L) f_R^n(\pi, c_j^R) + \text{H.c.}, \quad (24)$$

where $\langle H \rangle = v_W = 174$ GeV is the VEV acquired by the Higgs field. The zero modes give rise to the SM mass terms, and the resulting mass matrix reads

$$(M_f^{\text{RS}})_{ij} = v_W \frac{\lambda_{5,ij}^f}{kr_c \pi} f_L^0(\pi, c_{f_i}^L) f_R^0(\pi, c_{f_j}^R) \equiv v_W \frac{\lambda_{5,ij}^f}{kr_c \pi} F_L(c_{f_i}^L) F_R(c_{f_j}^R), \quad f = u, d, \quad (25)$$

where the label f denotes up-type or down-type quark species. Note that the Yukawa couplings are in general complex, and so take the form $\lambda_{5,ij}^f \equiv \rho_{ij}^f e^{i\phi_{ij}}$, with ρ_{ij}^f , ϕ_{ij} the magnitude and the phase, respectively.

III. STRUCTURE OF THE QUARK MASS MATRICES

In this section, we investigate the possible quark flavor structure in the RS framework. One immediate requirement on the candidate structures is that the experimentally observed quark mass spectrum and mixing pattern are reproduced. Another would be that the 5D Yukawa couplings are all of the same order, in accordance with the philosophy of the RS framework that there is no intrinsic hierarchy. We also required that constraints from EWPT are satisfied.

To arrive at the candidate structures, we follow two strategies. One is to start with a known SM quark mass matrix ansatz which reproduces the observed quark mass spectrum and mixing pattern. The ansatz form is then matched onto the RS mass matrix to see if the above requirements are satisfied. The other strategy is to generate RS mass matrices at random and then pick out those that satisfy the requirements above.¹

To solve the hierarchy problem, we take $kr_c = 11.7$ and the warped down scale to be $\tilde{k} = ke^{-kr_c\pi} = 1.65$ TeV.

¹This has been tried before in Ref. [8], but it was done for the case with $m_{\text{KK}} > 10$ TeV where there is a little hierarchy.

Since new physics first arise at the TeV scale in the RS framework, it is also where experimental data are matched to the RS model below. We will assume that the CKM matrix evolves slowly between $\mu = M_Z$ and $\mu = 1$ TeV so that the PDG values can be adopted, and we will use the running quark mass central values at $\mu = 1$ TeV from Ref. [13].

A. Structure from mass matrix ansatz

In trying to understand the pattern of quark flavor mixing, many ansatz for the SM quark mass matrices have been proposed over the years. There are two common types of mass matrix ansatz consistent with the current CKM data. One type is the Hermitian ansatz first proposed by Fritzsch some time ago [14], which has been recently updated to better accommodate $|V_{cb}|$ [15]. The other type is the symmetric ansatz proposed by Koide *et al.* [16], which was inspired by the nearly bimaximal mixing pattern in the lepton sector.² Using these ansatz as templates, we find that only the Koide-type ansatz admit hierarchy-free 5D Yukawa couplings; this property is demonstrated below. That Fritzsch-type ansatz generically lead to hierarchical Yukawa couplings is shown in Appendix A.

The admissible ansatz we found takes the form

$$M_f = P_f^\dagger \hat{M}_f P_f, \quad f = u, d, \quad (26)$$

where $P_f = \text{diag}\{e^{i\delta_1^f}, e^{i\delta_2^f}, e^{i\delta_3^f}\}$ is a diagonal pure phase matrix, and

$$\hat{M}_f = \begin{pmatrix} \xi_f & C_f & C_f \\ C_f & A_f & B_f \\ C_f & B_f & A_f \end{pmatrix}, \quad (27)$$

with all entries real and ξ_f much less than all other entries. When $\xi_f = 0$, the ansatz of Ref. [16] is recovered.

The real symmetric matrix \hat{M}_f is diagonalized by the orthogonal matrix

$$O_f^T \hat{M}_f O_f = \begin{pmatrix} \lambda_1^f & 0 & 0 \\ 0 & \lambda_2^f & 0 \\ 0 & 0 & \lambda_3^f \end{pmatrix}, \quad (28)$$

$$O_f = \begin{pmatrix} c_f & 0 & s_f \\ -\frac{s_f}{\sqrt{2}} & -\frac{1}{\sqrt{2}} & \frac{c_f}{\sqrt{2}} \\ -\frac{s_f}{\sqrt{2}} & \frac{1}{\sqrt{2}} & \frac{c_f}{\sqrt{2}} \end{pmatrix},$$

where the eigenvalues are given by

²In the SM, because of the freedom in choosing the RH flavor rotation, quark mass matrices can always be made Hermitian. But this need not be the case in the RS framework as we show below.

$$\begin{aligned}\lambda_1^f &= \frac{1}{2}[A_f + B_f + \xi_f - \sqrt{8C_f^2 + (A_f + B_f - \xi_f)^2}], \\ \lambda_2^f &= A_f - B_f, \\ \lambda_3^f &= \frac{1}{2}[A_f + B_f + \xi_f + \sqrt{8C_f^2 + (A_f + B_f - \xi_f)^2}],\end{aligned}\quad (29)$$

and the mixing angles are given by

$$c_f = \sqrt{\frac{\lambda_3^f - \xi_f}{\lambda_3^f - \lambda_1^f}}, \quad s_f = \sqrt{\frac{\xi_f - \lambda_1^f}{\lambda_3^f - \lambda_1^f}}. \quad (30)$$

Note that the components of \hat{M}_f can be expressed as

$$\begin{aligned}A_f &= \frac{1}{2}(\lambda_3^f - \lambda_2^f + \lambda_1^f - \xi_f), \\ B_f &= \frac{1}{2}(\lambda_3^f + \lambda_2^f + \lambda_1^f - \xi_f), \\ C_f &= \frac{1}{2}\sqrt{(\lambda_3^f - \xi_u)(\xi_u - \lambda_1^f)}.\end{aligned}\quad (31)$$

To reproduce the observed mass spectrum $m_1^f < m_2^f < m_3^f$, the eigenvalues λ_i^f , $i = 1, 2, 3$, are assigned to be the appropriate quark masses. For the Koide ansatz (the $\xi_f = 0$ case), it was pointed out in Ref. [17] that different assignments are needed for the up and down sectors to fit $|V_{ub}|$ better. Since the ansatz, Eq. (26), is really a perturbed Koide ansatz, we follow the same assignments here:

$$\begin{aligned}\lambda_1^u &= -m_1^u, & \lambda_2^u &= m_2^u, & \lambda_3^u &= m_3^u, \\ \lambda_1^d &= -m_1^d, & \lambda_2^d &= m_3^d, & \lambda_3^d &= m_2^d.\end{aligned}\quad (32)$$

Now since $O_d^T \hat{M}_d O_d = \text{diag}\{-m_1^d, m_3^d, m_2^d\}$ for the down-type quarks, to put the eigenvalues into hierarchical order, the diagonalization matrix becomes $O_d^l = O_d T_{23}$, where

$$T_{23} = \begin{pmatrix} 1 & 0 & 0 \\ 0 & 0 & 1 \\ 0 & 1 & 0 \end{pmatrix}. \quad (33)$$

The quark mixing matrix is then given by

$$\begin{aligned}V_{\text{mix}} &= O_u^T P_u P_d^\dagger O_d^l \\ &= \begin{pmatrix} c_u c_d + \kappa s_u s_d & c_u s_d - \kappa s_u c_d & -\sigma s_u \\ -\sigma s_d & \sigma c_d & \kappa \\ s_u c_d - \kappa c_u s_d & s_u s_d + \kappa s_u s_d & -\sigma c_u \end{pmatrix},\end{aligned}\quad (34)$$

where

$$\begin{aligned}\kappa &= \frac{1}{2}(e^{i\delta_3} + e^{i\delta_2}), & \sigma &= \frac{1}{2}(e^{i\delta_3} - e^{i\delta_2}), \\ \delta_i &= \delta_i^u - \delta_i^d, & i &= 1, 2, 3.\end{aligned}\quad (35)$$

Without loss of generality, δ_1 is taken to be zero.

The matrix V_{mix} depends on four free parameters, $\delta_{2,3}$ and $\xi_{u,d}$. A good fit to the CKM matrix is found by demanding the following set of conditions:

$$\begin{aligned}|\kappa| &= |V_{cb}| = 0.04160, & |\sigma|s_u &= |V_{ub}| = 0.00401, \\ |\sigma|s_d &= |V_{cd}| = 0.22725,\end{aligned}\quad (36)$$

and $\delta_{CP} = -(\delta_3 + \delta_2)/2 = 59^\circ$. These imply

$$\begin{aligned}\delta_2 &= -2.55893, & \delta_3 &= -0.49944, \\ \xi_u &= 1.36226 \times 10^{-3}, & \xi_d &= 6.50570 \times 10^{-5},\end{aligned}\quad (37)$$

which in turn lead to a Jarlskog invariant of $J = 3.16415 \times 10^{-5}$ and

$$|V_{\text{mix}}| = \begin{pmatrix} 0.97380 & 0.22736 & 0.00401 \\ 0.22725 & 0.97294 & 0.04160 \\ 0.00816 & 0.04099 & 0.99913 \end{pmatrix}, \quad (38)$$

both of which are in very good agreement with the globally fitted data.

With $\delta_{u,d}$ determined, so are $\hat{M}_{u,d}$ also. From Eq. (31) we have

$$\begin{aligned}A_u &= 77.32226, & A_d &= 1.26269, \\ B_u &= 76.77526, & B_d &= -1.21731, \\ C_u &= 0.43733, & C_d &= 7.91684 \times 10^{-3}.\end{aligned}\quad (39)$$

Parameters of the RS mass matrix (25) can now be solved for by matching the RS mass matrix onto the ansatz (26). Starting with M_u^{RS} , there are a total of 24 parameters to be determined: six fermion wave function values, $F_L(c_{Q_i})$ and $F_R(c_{U_i})$, nine Yukawa magnitudes, ρ_{ij}^u , and nine Yukawa phases, ϕ_{ij}^u , where $i, j = 1, 2, 3$.³ Matching M_u^{RS} to M_u results in nine conditions for both magnitudes and phases. Thus all the up-type Yukawa phases are determined by the three phases δ_i^u , while six magnitudes are left as free independent parameters. These we chose to be $F_L(c_{Q_3})$ and $F_R(c_{U_3})$, which are constrained by EWPT, and ρ_{11}^u , ρ_{21}^u , ρ_{31}^u , ρ_{32}^u .

Next we match M_d^{RS} to M_d . Since $F_L(c_{Q_i})$ have already been determined, there are only 21 parameters left in M_d^{RS} : $F_R(c_{D_i})$, ρ_{ij}^d , and ϕ_{ij}^d . Again all the down-type Yukawa phases are determined by the three phases, δ_i^d , leaving three free magnitudes which we chose to be ρ_{31}^d , ρ_{32}^d , and ρ_{33}^d . We collect all relevant results from the matching processes into Appendix B.

To see that the ansatz (26) does not lead to a hierarchy in the Yukawa couplings, note from Eq. (31) we have

$$A_f \sim |B_f| \sim \frac{m_3^f}{2}, \quad C_u \sim \frac{\sqrt{m_3^u m_1^u}}{2}, \quad C_d \sim \frac{\sqrt{m_2^d m_1^d}}{2}. \quad (40)$$

³We will denote using subscripts Q , U , and D respectively, for the left-handed quark doublet, and the right-handed up- and down-type singlets of $SU(2)_L$.

Given this and Eq. (37), we see from Eqs. (B1) and (B4) that as long as

$$\rho_{31}^d \sim \rho_{32}^d \sim \rho_{33}^d \sim \rho_{11}^u \sim \rho_{21}^u \sim \rho_{31}^u \sim \rho_{32}^u \sim \rho_{33}^u, \quad (41)$$

all Yukawa couplings would be of the same order in magnitude. It is amusing to note that if we begin by imposing the condition that the 5D Yukawa couplings are hierarchy-free instead of first fitting the CKM data, we find

$$\xi_u \sim m_1^u \sim 10^{-3}, \quad \xi_d \sim \sqrt{m_2^d m_1^d} \sqrt{\frac{m_1^u}{m_3^u}} \sim 3 \times 10^{-5}, \quad (42)$$

which give the correct order of magnitude for $\xi_{u,d}$ necessary for V_{mix} to fit the experimental CKM values.

From relations (B1), (B3), and (B6), for mass matrices given by the ansatz (26), all localization parameters can be determined from just that of the third generation $SU(2)_L$ doublet, c_{Q_3} , and the Yukawa coupling magnitudes listed in Eq. (41). To satisfy the bounds from flavor-changing neutral-currents (FCNCs), LH light quarks from the first two generations should be localized towards the UV brane. As discussed in Appendix B, for generic choices of Yukawa couplings this is so for the first generation LH quarks, but not for the second generation. In order to have $c_{Q_2} > 0.5$ while still satisfying constraints from Eqs. (B8) and (B9) and the EWPT constraint $c_{U_3} < 0.2$, we choose

$$\frac{\rho_{31}^u}{\rho_{21}^u} = 0.2615, \quad \rho_{11}^u = \rho_{31}^u = 0.7, \quad \rho_{33}^u = 0.85, \\ \rho_{32}^u = \rho_{31}^d = \rho_{31}^d = \rho_{33}^d = 1. \quad (43)$$

We also have to shorten the EWPT allowed range of c_{Q_3} to (0.3, 0.4) so that $c_{Q_2} > 0.5$ is always satisfied. Note that relation (B3) constrains c_{U_2} to be greater than -0.5 if the perturbativity constraint, $\lambda_5 < 4$, is to be met.

The localization parameters increase monotonically as c_{Q_3} increases. Except for $c_{U_{2,3}}$, the variation of the localization parameters is small. We list below their range variation as c_{Q_3} varies from 0.3 to 0.4 given the choice of the Yukawa couplings (43):

$$0.65 < c_{Q_1} < 0.66, \quad 0.50 < c_{Q_2} < 0.52, \\ -0.62 < c_{U_1} < -0.61, \quad -0.26 < c_{U_2} < -0.01, \\ -0.16 < c_{U_3} < 0.18, \quad -0.75 < c_{D_1} < -0.74, \\ -0.60 < c_{D_{2,3}} < -0.59. \quad (44)$$

B. Structure from numerical search

The RS mass matrix given by Eq. (25) has a productlike form:

$$M^{\text{RS}} \sim \begin{pmatrix} a_1 b_1 & a_1 b_2 & a_1 b_3 \\ a_2 b_1 & a_2 b_2 & a_2 b_3 \\ a_3 b_1 & a_3 b_2 & a_3 b_3 \end{pmatrix}, \quad (45) \\ a_i = F_L(c_i^L), \quad b_i = F_R(c_i^R),$$

and it can be brought into the diagonal form by a unitary transformation

$$(U_L^f)^\dagger M_f^{\text{RS}} U_R^f = \begin{pmatrix} \lambda_1^f & 0 & 0 \\ 0 & \lambda_2^f & 0 \\ 0 & 0 & \lambda_3^f \end{pmatrix}, \quad f = u, d. \quad (46)$$

Suppose there is just one universal 5D Yukawa coupling, say $\lambda_5 = 1$, then the RS mass matrix M_f^{RS} would be singular with two zero eigenvalues, and both the LH and RH quark mixing matrices would be the identity matrix, i.e. $V_{\text{mix}}^{L,R} = (U_{L,R}^u)^\dagger U_{L,R}^d = \mathbb{1}_{3 \times 3}$. Thus, in order to obtain realistic quark masses and CKM mixing angles ($V_{\text{mix}}^L \equiv V_{\text{CKM}}$), one cannot assume one universal Yukawa coupling. Rather, for each configuration of localization parameters, the magnitudes and phases of the 5D Yukawa coupling constants, ρ_{ij} and ϕ_{ij} , will be randomly chosen from the intervals [1.0, 3.0] and $[0, 2\pi]$ respectively, and we take a sample size of 10^5 .

The numerical search is done with $0.5 < c_{Q_{1,2}} < 1$ and $-1 < c_{U_{1,2}}, c_{D_{1,2,3}} < -0.5$ so that the first two generation quarks, as well as the third generation RH quarks of the D_3 doublet are localized towards the UV brane. For the third generation, $0.25 < c_{Q_3} < 0.4$ and $-0.5 < c_{U_3} < 0.2$ are required so the EWPT constraints are satisfied (see Appendix B). We averaged the quark masses and CKM mixing angles over the entire sample for each configuration of localization parameters, and these choices yielded averaged values that are within one statistical deviation of the experimental values at $\mu = 1$ TeV as given in Ref. [13]. Below we give three representative configurations from the admissible configurations found after an extensive search.

(i) Configuration I:

$$c_Q = \{0.634, 0.556, 0.256\}, \\ c_U = \{-0.664, -0.536, 0.185\}, \quad (47) \\ c_D = \{-0.641, -0.572, -0.616\}.$$

In units of GeV, the mass matrices averaged over the whole sample are given by

$$\langle |M_u| \rangle = \begin{pmatrix} 8.97 \times 10^{-4} & 0.049 & 0.767 \\ 0.010 & 0.554 & 8.69 \\ 0.166 & 9.06 & 142.19 \end{pmatrix}, \quad (48) \\ \langle |M_d| \rangle = \begin{pmatrix} 0.0019 & 0.017 & 0.0044 \\ 0.022 & 0.196 & 0.050 \\ 0.352 & 3.209 & 0.813 \end{pmatrix},$$

which have eigenvalues

$$\begin{aligned}
 m_t &= 109(52), & m_b &= 2.59 \pm 1.11, \\
 m_c &= 0.56(59), & m_s &= 0.048(32), \\
 m_u &= 0.0011(12), & m_d &= 0.0017(12).
 \end{aligned} \tag{49}$$

The resulting mixing matrices are given by

$$\begin{aligned}
 |V_{us}^L| &= 0.16(14), & |V_{us}^R| &= 0.42(24), \\
 |V_{ub}^L| &= 0.009(11), & |V_{ub}^R| &= 0.12(10), \\
 |V_{cb}^L| &= 0.079(74), & |V_{cb}^R| &= 0.89(13),
 \end{aligned} \tag{50}$$

which give rise to an averaged Jarlskog invariant consistent with zero with a standard error of 1.3×10^{-4} .

(ii) Configuration II:

$$\begin{aligned}
 c_Q &= \{0.629, 0.546, 0.285\}, \\
 c_U &= \{-0.662, -0.550, 0.080\}, \\
 c_D &= \{-0.580, -0.629, -0.627\}.
 \end{aligned} \tag{51}$$

In units of GeV, the mass matrices averaged over the entire sample are given by

$$\begin{aligned}
 \langle |M_u| \rangle &= \begin{pmatrix} 0.0011 & 0.039 & 0.834 \\ 0.014 & 0.492 & 10.55 \\ 0.16 & 5.726 & 122.87 \end{pmatrix}, \\
 \langle |M_d| \rangle &= \begin{pmatrix} 0.017 & 0.0034 & 0.0036 \\ 0.209 & 0.043 & 0.046 \\ 2.43 & 0.506 & 0.539 \end{pmatrix},
 \end{aligned} \tag{52}$$

which have eigenvalues

$$\begin{aligned}
 m_t &= 95(45), & m_b &= 2.01(83), \\
 m_c &= 0.49(50), & m_s &= 0.057(35), \\
 m_u &= 0.0014(16), & m_d &= 0.0022(15).
 \end{aligned} \tag{53}$$

The resulting mixing matrices are given by

$$\begin{aligned}
 |V_{us}^L| &= 0.14(12), & |V_{us}^R| &= 0.30(20), \\
 |V_{ub}^L| &= 0.011(13), & |V_{ub}^R| &= 0.90(12), \\
 |V_{cb}^L| &= 0.11(10), & |V_{cb}^R| &= 0.23(15),
 \end{aligned} \tag{54}$$

which give rise to an averaged Jarlskog invariant consistent with zero with a standard error of 2.3×10^{-4} .

(iii) Configuration III:

$$\begin{aligned}
 c_Q &= \{0.627, 0.571, 0.272\}, \\
 c_U &= \{-0.518, -0.664, 0.180\}, \\
 c_D &= \{-0.576, -0.610, -0.638\},
 \end{aligned} \tag{55}$$

In units of GeV, the mass matrices averaged over the entire sample are given by

$$\begin{aligned}
 \langle |M^u| \rangle &= \begin{pmatrix} 0.092 & 0.0010 & 0.940 \\ 0.554 & 0.0065 & 5.66 \\ 13.4 & 0.158 & 136.9 \end{pmatrix}, \\
 \langle |M^d| \rangle &= \begin{pmatrix} 0.019 & 0.0066 & 0.0026 \\ 0.114 & 0.039 & 0.016 \\ 2.774 & 0.955 & 0.376 \end{pmatrix},
 \end{aligned} \tag{56}$$

which have eigenvalues

$$\begin{aligned}
 m_t &= 106(50), & m_b &= 2.32(94), \\
 m_c &= 0.56(55), & m_s &= 0.036(21), \\
 m_u &= 0.0013(12), & m_d &= 0.0023(16).
 \end{aligned} \tag{57}$$

The resulting mixing matrices are given by

$$\begin{aligned}
 |V_{us}^L| &= 0.27(19), & |V_{us}^R| &= 0.77(19), \\
 |V_{ub}^L| &= 0.010(10), & |V_{ub}^R| &= 0.36(21), \\
 |V_{cb}^L| &= 0.048(44), & |V_{cb}^R| &= 0.85(15),
 \end{aligned} \tag{58}$$

which give rise to an averaged Jarlskog invariant consistent with zero with a standard error of 1.9×10^{-4} .

In summary, from the numerical study we found that, in the RS framework, there is neither a preferred form for the mass matrix nor a universal RH mixing pattern. Note that the RH mixing matrix is in general quite different from its LH counterpart, viz. the CKM matrix.

IV. FLAVOR VIOLATING TOP QUARK DECAYS

In this section we study the consequences the different forms of quark mass matrices have on FCNC processes. We focus below on the decay, $t \rightarrow c(u)Z \rightarrow c(u)l\bar{l}$, where $l = e, \mu, \tau, \nu$. Modes which decay into a real Z and $c(u)$ jets are expected to have a much higher rate than those involving a photon or a light Higgs, which happen through loop effects. Moreover, much cleaner signatures at the LHC can be provided by leptonic Z decays.

A. Tree-level flavor violations in MCRS

Tree-level FCNCs are generic in extradimensional models, for both a flat background geometry [18] and a warped one [8,19,20]. Because of the KK interactions, the couplings of the Z to the fermions are shifted from their SM values. These shifts are not universal in general, and so flavor violations necessarily result when the fermions are rotated from the weak to the mass eigenbasis.

More concretely, consider the $Zf\bar{f}$ coupling in the weak eigenbasis:

$$\begin{aligned}
 \mathcal{L}_{\text{NC}} \supset & g_Z Z_\mu \left\{ Q_Z(f_L) \sum_{i,j} (\delta_{ij} + \kappa_{ij}^L) \bar{f}_{iL} \gamma^\mu f_{jL} \right. \\
 & \left. + Q_Z(f_R) \sum_{i,j} (\delta_{ij} + \kappa_{ij}^R) \bar{f}_{iR} \gamma^\mu f_{jR} \right\},
 \end{aligned} \tag{59}$$

where i, j are family indices, $\kappa_{ij} = \text{diag}(\kappa_1, \kappa_2, \kappa_3)$, and

$$Q_Z(f) = T_L^3(f) - s^2 Q_f, \quad (60)$$

$$Q_f = T_L^3(f) + T_R^3(f) + Q_X(f) = T_L^3(f) + \frac{Y_f}{2},$$

where Q_f is the electric charge of the fermion, $Y_f/2$ the hypercharge, $T_{L,R}(f)$ the weak isospin under $SU(2)_{L,R}$, and $Q_X(f)$ the charge under $U(1)_X$. We define $\kappa_{ij} \equiv \delta g_{i,j}^{L,R}/g_Z$ to be the shift in the weak eigenbasis Z couplings to fermions relative to its SM value given by $g_Z \equiv e/(sc)$, as well as the usual quantities

$$e = \frac{g_L g'}{\sqrt{g_L^2 + g'^2}}, \quad g' = \frac{g_R g_X}{g_R^2 + g_X^2}, \quad (61)$$

$$s = \frac{e}{g_L}, \quad c = \sqrt{1 - s^2},$$

where $g_L = g_{5L}/\sqrt{r_c \pi}$ is the 4D gauge coupling constant of $SU(2)_L$ (and similarly for the rest). Rotating to the mass eigenbasis of the SM quarks defined by $f' = U^\dagger f$, where the unitary matrix U diagonalizes the SM quark mass matrix, flavor off-diagonal terms appear:

$$\mathcal{L}_{\text{FCNC}} \supset g_Z Z_\mu \left\{ Q_Z(f_L) \sum_{a,b} \hat{\kappa}_{ab}^L \bar{f}'_{aL} \gamma^\mu f'_{bL} + Q_Z(f_R) \sum_{a,b} \hat{\kappa}_{ab}^R \bar{f}'_{aR} \gamma^\mu f'_{bR} \right\}, \quad (62)$$

where the mass eigenbasis flavor off-diagonal couplings are given by

$$\hat{\kappa}_{ab}^{L,R} = \sum_{i,j} (U_{L,R}^\dagger)_{ai} \kappa_{ij}^{L,R} (U_{L,R})_{jb}. \quad (63)$$

Note that the off-diagonal terms would vanish only if κ is proportional to the identity matrix.

In the RS framework, one leading source of corrections to the SM neutral current interaction comes from the exchanges of heavy KK neutral gauge bosons as depicted in Fig. 1. The effect of gauge KK exchanges gives rise only to the diagonal terms of κ . It can be efficiently calculated with the help of the massive gauge 5D mixed position-

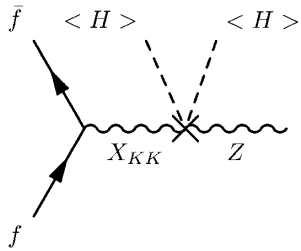


FIG. 1. Correction to the $Zf\bar{f}$ coupling due to the exchange of gauge KK modes. The fermions are in the weak eigenbasis, and $X = Z, Z'$.

momentum space propagators, which automatically sums up contributions from all the KK modes [11,21].

The leading contributions can be computed in terms of the overlap integral,

$$G_f^{L,R}(c_{L,R}) = \frac{v_W^2}{2} r_c \int_0^\pi d\phi |f_{L,R}^0(\phi, c_{L,R})|^2 \tilde{G}_{p=0}(\phi, \pi), \quad (64)$$

where $\tilde{G}_{p=0}$ is the zero-mode subtracted gauge propagator evaluated at zero 4D momentum. For KK modes obeying the $(++)$ boundary condition, $\tilde{G}_{p=0}$ is given by [21]

$$\tilde{G}_{p=0}^{(++)}(\phi, \phi') = \frac{1}{4k(kr_c \pi)} \left\{ \frac{1 - e^{2kr_c \pi}}{kr_c \pi} + e^{2kr_c \phi} (1 - 2kr_c \phi) + e^{2kr_c \phi'} [1 + 2kr_c (\pi - \phi')] \right\}, \quad (65)$$

and those obeying the $(-+)$ boundary condition

$$\tilde{G}_{p=0}^{(-+)}(\phi, \phi') = -\frac{1}{2k} (e^{2kr_c \phi} - 1), \quad (66)$$

where $\phi_<$ ($\phi_>$) is the minimum (maximum) of ϕ and ϕ' . The gauge KK correction to the Z coupling is thus $\kappa_{ij}^g = \kappa_{q_i}^g \delta_{ij}$, with $\kappa_{q_i}^g$ given by [22]

$$(\kappa_{q_i}^g)_{L,R} = \frac{e^2}{s^2 c^2} \left\{ G_{++}^{q_{L,R}} - \frac{G_{-+}^{q_{L,R}}}{Q_Z(q_{L,R}^i)} \times \left[\frac{g_R^2}{g_L^2} c^2 T_R^3(q_{L,R}^i) - s^2 \frac{Y_{q_{L,R}^i}}{2} \right] \right\}, \quad (67)$$

where the label q denotes the fermion species. Note that when the fermions are localized towards the UV brane ($c_L \gtrsim 0.6$ and $c_R \lesssim -0.6$), G_{-+} is negligible, while G_{++} becomes essentially flavor independent [22].

Another source of corrections to the $Zf\bar{f}$ coupling arises from the mixings between the fermion zero modes and the fermion KK modes brought about by the Yukawa interactions. These generate diagonal as well as off-diagonal terms in κ . The diagram involved is depicted in Fig. 2.

The effects of the fermion mixings may be similarly calculated by using the fermion analogue of the gauge propagators. It is however much more convenient to deal

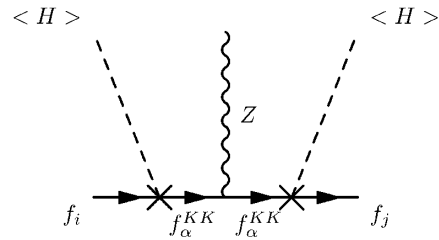


FIG. 2. Correction to the $Zf\bar{f}$ coupling due to SM fermions mixing with the KK modes. The fermions are in the weak eigenbasis.

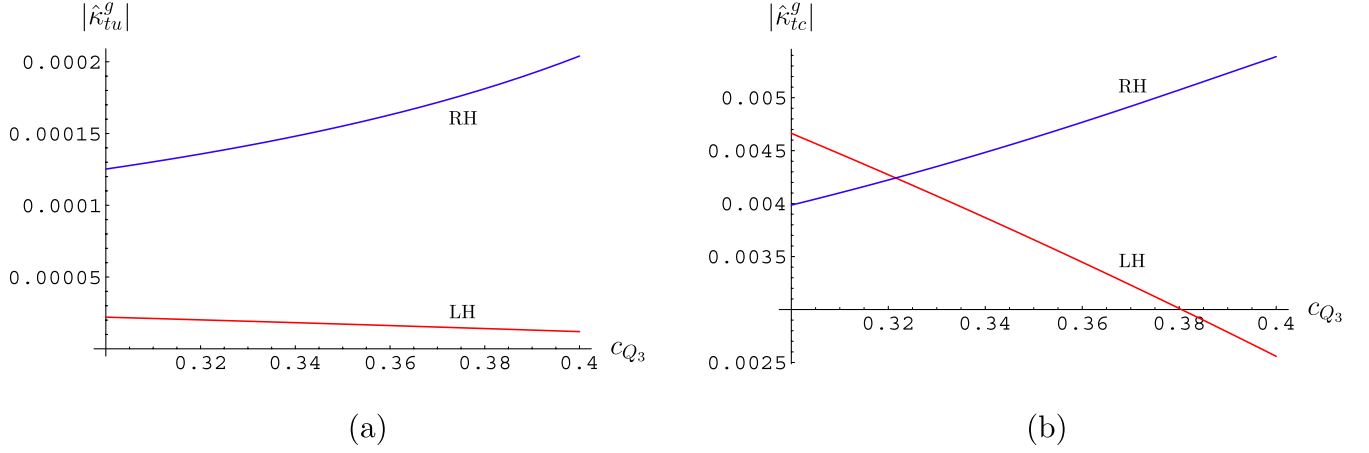


FIG. 3 (color online). Gauge KK contribution in the case of symmetrical mass matrices to (a) $\hat{\kappa}_{tu}^g$ and (b) $\hat{\kappa}_{tc}^g$. The labels LH and RH indicate whether it is for the LH or RH coupling.

directly with the KK modes here. The KK fermion corrections to the weak eigenbasis Z couplings can be written as

$$\begin{aligned}
 (\kappa_{ij}^f)_L &= \sum_{\alpha} \sum_{n=1}^{\infty} \frac{m_{i\alpha}^* m_{j\alpha}}{(m_n^{\alpha})^2} \tilde{\delta}_R^{\alpha}, \\
 (\kappa_{ij}^f)_R &= \sum_{\alpha} \sum_{n=1}^{\infty} \frac{m_{\alpha i} m_{\alpha j}^*}{(m_n^{\alpha})^2} \tilde{\delta}_L^{\alpha},
 \end{aligned} \tag{68}$$

where m_n is the n th level KK fermion mass, $m_{i\alpha}$ are entries of the weak eigenbasis RS mass matrix (25) with α a generation index,⁴ and

$$\tilde{\delta}_{R,L}^{\alpha} = \left| \frac{f_{R,L}^n(\pi, c_{\alpha}^{R,L})}{f_{R,L}^0(\pi, c_{\alpha}^{R,L})} \right|^2 \frac{Q_Z(f_{R,L})}{Q_Z(f_{L,R})}, \tag{69}$$

with the argument of Q_Z , $f = u, d$, denoting up-type or down-type quark species. Note that for $c_{\alpha}^L < 1/2$ and $c_{\alpha}^R > -1/2$, $|f_{L,R}^n(\pi, c_{\alpha}^{L,R})| \approx \sqrt{2kr_c \pi}$.

To determine $\hat{\kappa}_{ab}$ in Eq. (63), one needs to know the rotation matrices U_L and U_R . In the case where the weak eigenbasis mass matrices are given by the symmetric ansatz (26), the analytical form of the rotation matrices is known. By rephasing the quark fields so that $\delta_i^u = 0$ and all the Yukawa phases reside in down sector, the up-type rotation matrix is just the orthogonal diagonalization matrix given by Eq. (28). Using the solution of the CKM fit given in Eq. (37), we have

⁴For shift in the LH couplings, the index α runs over the generations of both types of $SU(2)_R$ doublets, U and D , both of which contain KK modes that can mix with LH zero modes. For shift in the RH couplings, α runs over just the generations of the only type of $SU(2)_L$ doublets, Q .

$$U_L^u = U_R^u = U^u,$$

$$U^u = O_u = \begin{pmatrix} 0.99999 & 0 & 0.00401 \\ -0.00284 & -\frac{1}{\sqrt{2}} & 0.70710 \\ -0.00284 & \frac{1}{\sqrt{2}} & 0.70710 \end{pmatrix}. \tag{70}$$

Since we are interested in flavor violating top decays, the relevant mass eigenbasis off-diagonal corrections are $\hat{\kappa}_{3r} = \hat{\kappa}_{3r}^g + \hat{\kappa}_{3r}^f$, $r = 1, 2$. For the discussion below, using relations (B1), (B3), and (B6) we will trade the dependences of $\hat{\kappa}_{ab}^{L,R}$ on all the different localization parameters for just a single dependence on c_{Q_3} , and the Yukawa coupling magnitudes which we fix to take the values given in Eq. (43). Recall that with this choice of the Yukawa coupling magnitudes, the EWPT allowed range for c_{Q_3} is between 0.3 and 0.4.

Since $\kappa_{ij}^g = \kappa_{q_i}^g \delta_{ij}$, the gauge KK contributions is simply $\hat{\kappa}_{3r}^g = \sum_i \kappa_{q_i}^g (U^u)_{3i}^{\dagger} U_{ir}^u$, with

$$\begin{aligned}
 \hat{\kappa}_{tu}^g &= 2.00672 \times 10^{-3} (2\kappa_u^g - \kappa_c^g - \kappa_t^g), \\
 \hat{\kappa}_{tc}^g &= 0.50(\kappa_t^g - \kappa_c^g).
 \end{aligned} \tag{71}$$

We plot $\hat{\kappa}_{3r}^g$ as a function of c_{Q_3} in Fig. 3.

For the fermion KK contributions, since the decoupling of the higher KK modes is very efficient, hence just the first KK mode provides a very good approximation to the full tower. We plot using this approximation $|\hat{\kappa}_{3r}^f|$ as functions of c_{Q_3} in Fig. 4.

B. Experimental signatures at the LHC

The branching ratio of the decay $t \rightarrow c(u)Z$ is given by

$$\begin{aligned}
 \text{Br}(t \rightarrow c(u)Z) &= \frac{2}{c^2} (|Q_Z(t_L) \hat{\kappa}_{tc(u)}^L|^2 + |Q_Z(t_R) \hat{\kappa}_{tc(u)}^R|^2) \\
 &\quad \times \left(\frac{1-x_t}{1-y_t} \right)^2 \left(\frac{1+2x_t}{1+2y_t} \right) \frac{y_t}{x_t},
 \end{aligned} \tag{72}$$

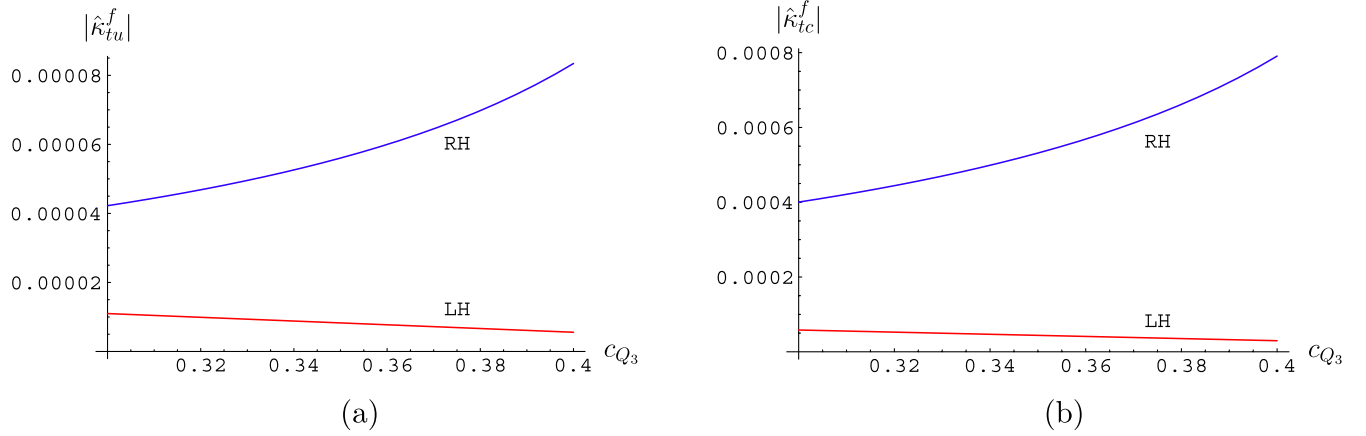


FIG. 4 (color online). Fermion KK contribution in the case of symmetrical mass matrices to (a) $\hat{\kappa}_{tu}$ and (b) $\hat{\kappa}_{tc}$. The labels LH and RH indicate whether it is for the LH or RH coupling. The plots are made using the first KK mode to approximate the full KK tower.

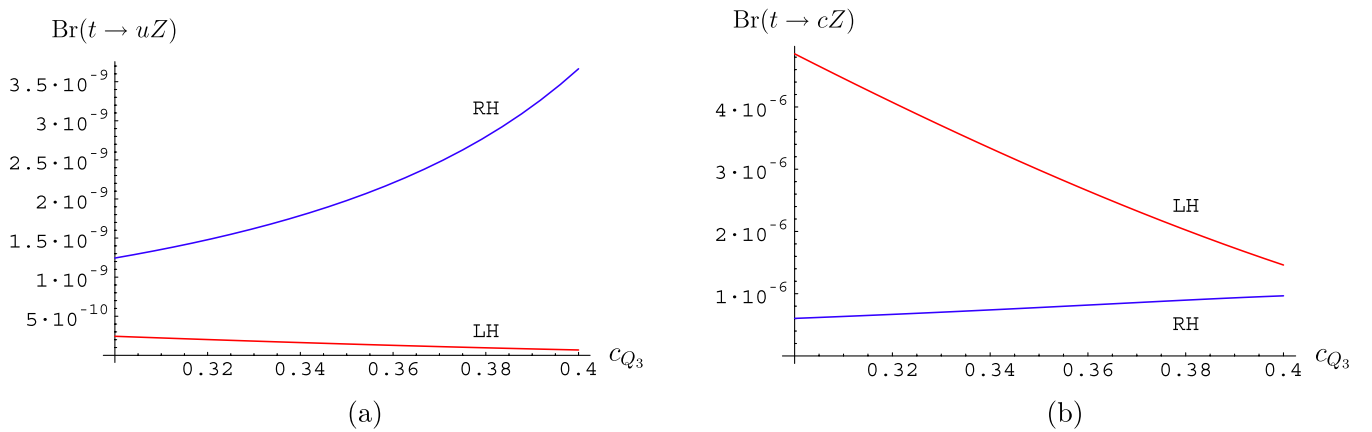


FIG. 5 (color online). Branching ratio in the case of symmetrical mass matrices as a function of c_{Q_3} for the decay (a) $t \rightarrow uZ$ and (b) $t \rightarrow cZ$. The labels LH and RH indicate LH or RH top decay.

where $x_t = m_Z^2/m_t^2$ and $y_t = m_W^2/m_t^2$. In Fig. 5 we plot the branching ratio as a function of c_{Q_3} in the case where the weak eigenbasis mass matrix has the symmetric ansatz form of (26). It is clear that the dominant channel is $t \rightarrow cZ$. The branching ratio is at the level of a few 10^{-6} , which is to be compared to the SM prediction of $\mathcal{O}(10^{-13})$ [23]. As c_{Q_3} increases, the decay changes from being mostly coming from the LH tops at the low end of the allowed range of c_{Q_3} , to having comparable contributions from both quark helicities at the high end. Note that one can in principle differentiate whether the quark rotation is LH or RH by studying the polarized top decays.

For the case of asymmetrical quark mass matrix configurations found in Sec. III B, the resultant branching ratios and the associated gauge and fermion KK flavor off-diagonal contributions are tabulated in Table I. We give results only for the decay into charm quarks since this channel dominates over that into the up-quarks. The magnitude of our branching ratios for both cases of symmetrical and asymmetrical quark mass matrices is consistent with the previous estimate in the RS framework [24].

It is interesting to note from Fig. 5(b) and Table I that, in $t \rightarrow cZ$ decays, the LH decays dominate over the RH ones in the case of both symmetrical and asymmetrical quark mass matrices. The reason for this is however different for the two cases. In the symmetric case, $M_u = M_u^\dagger$ and so $U_L^u = U_R^u = U^u$. Thus the difference between the LH and RH decays is due to the differences in the weak eigenbasis couplings, as can be seen from Eq. (71), and Q_Z . By comparing Fig. 4(b) to 3(b) we see $|\hat{\kappa}_{tc}^f| \sim |\hat{\kappa}_{tc}^g|$, and from Fig. 3(b) we have $0.9 \lesssim |(\hat{\kappa}_{tc}^g)_R|/|(\hat{\kappa}_{tc}^g)_L| \lesssim 2$.⁵

⁵It may seem counterintuitive that $|(\hat{\kappa}_{tc}^g)_R|$ can be smaller than $|(\hat{\kappa}_{tc}^g)_L|$ (for $c_{Q_3} < 0.32$), as one may expect that the couplings to be dominated by the top contribution, and the coupling to the RH top to be larger than that to the LH top due to the fact that the RH top is localized closer to the IR brane. However, such expectations can be misleading. Because of the mixing matrices, the mass eigenbasis coupling, $\hat{\kappa}_{tc}^g$, is not just a simple sum of the weak eigenbasis couplings, $\kappa_{q_i}^g$, but involves their differences as already mentioned. Moreover, although the greatest contribution comes from the top, the contribution from the second generation may not be completely negligible, as is the case here for $(\kappa_c^g)_R$ for the particular symmetric ansatz that we study.

TABLE I. Branching ratios of $t \rightarrow cZ$ and the associated gauge and fermion KK flavor off-diagonal contributions for the case of asymmetrical mass matrices found from numerical searches.

Configuration	$ \hat{\kappa}_L^g $	$ \hat{\kappa}_R^g $	$ \hat{\kappa}_L^f $	$ \hat{\kappa}_R^f $	$\text{Br}(t_L)$	$\text{Br}(t_R)$
I	3.5×10^{-4}	7.7×10^{-3}	8.2×10^{-3}	4.7×10^{-3}	1.4×10^{-5}	4.1×10^{-6}
II	4.3×10^{-4}	5.8×10^{-3}	9.9×10^{-3}	2.9×10^{-3}	2.1×10^{-5}	2.0×10^{-6}
III	2.1×10^{-4}	3.8×10^{-3}	5.0×10^{-3}	7.0×10^{-3}	5.4×10^{-6}	3.2×10^{-6}

However, as $|Q_Z(t_L)| \gtrsim |2Q_Z(t_R)|$, the net effect is that the LH decay dominates [see Eq. (72)].

In the asymmetrical case, $M_u \neq M_u^\dagger$ and $U_L^u \neq U_R^u$ with no pattern relating the LH to the RH mixings. In each of the configurations of localization parameters listed in Table I, while $|(\hat{\kappa}_{ic}^g)_L| \ll |(\hat{\kappa}_{ic}^g)_R|$, it turns out that not only $|(\hat{\kappa}_{ic}^g)_R| \sim |(\hat{\kappa}_{ic}^f)_R|$ and $|(\hat{\kappa}_{ic}^f)_L| \sim |(\hat{\kappa}_{ic}^f)_R|$, there is also a relative minus sign between the gauge and the fermion KK contributions, which results in a destructive interference that leads to a greater branching ratio for the LH decay. This is to be contrasted with Ref. [24] where it is the RH mode that is found to dominate. There it appears that the possibility of having a cancellation between the gauge and fermion KK contributions was not considered.

We note and emphasize here the crucial role the quark mass and mixing matrices play in determining the mass eigenbasis flavor off-diagonal couplings $\hat{\kappa}_{ab}$. Most importantly, $\hat{\kappa}_{ab}$ do not depend on the fermion localizations alone. Whether or not there is a cancellation between the gauge and fermion KK contributions depends very much on the combination of the particular quark mass and mixing matrices considered just as well as the configuration of fermion localizations used. Such cancellation is by no mean generic, and has to be checked whenever a new combination of admissible configuration of fermion localizations, and quark mass and mixing matrices arise. In addition, since 5D gauge and Yukawa couplings are independent parameters, whether or not $|(\hat{\kappa}_{ab}^g)_L| \ll |(\hat{\kappa}_{ab}^g)_R|$ does not mean the same has to hold between $|(\hat{\kappa}_{ab}^f)_L|$ and $|(\hat{\kappa}_{ab}^f)_R|$. Since κ_{ij}^g and κ_{ij}^f have very different structures [see Eqs. (67) and (68)], the combined effect when convolved with the particular quark mixing matrices can be quite different, as is the case for the three asymmetrical configurations listed in Table I.

It is expected that both the single top and the $\bar{t}t$ pair production rates will be high at the LHC, with the latter about a factor of 2 higher still than the former. To a small correction, the single tops are always produced in the LH helicity, while both helicities are produced in pair productions. Thus a simple way of testing the above at the LHC is to compare the decay rates of $t \rightarrow Z + \text{jets}$ in single top production events (e.g. in the associated tW productions) to that from the pair productions, so that information of both LH and RH decays can be extracted. Note that both the single and pair production channels should give comparable branching ratios initially at the discovery stage. Of

course, a higher branching ratio would be obtained from pair productions after several years of measurements.

V. SUMMARY

We have performed a detailed study of the admissible forms of quark mass matrices in the MCRS model which reproduce the experimentally well-determined quark mass hierarchy and CKM mixing matrix, assuming a perturbative and hierarchyless Yukawa structure that is not fine-tuned.

We arrived at the admissible forms in two different ways. In one we examined several quark mass matrix ansatz which are constructed to fit the quark masses and the CKM matrix. These ansatz have a high degree of symmetries built in which allows the localization of the quarks (that give rise to the mass hierarchy in the RS setting) to be analytically determined. We found that the Koide-type symmetrical ansatz is compatible with the assumption of a hierarchyless Yukawa structure in the MCRS model, but not the Fritzsch-type Hermitian ansatz. Because the ansatzed mass matrices are symmetrical, both LH and RH quark mixing matrices are the same.

In the other way, no *a priori* quark mass structures were assumed. A numerical multiparameter search for configurations of quark localization parameters and Yukawa couplings that give admissible quark mass matrices was performed. Admissible configurations were found after an extensive search. No discernible symmetries or pattern were found in the quark mass matrices for both the up-type and down-type quarks. The LH and RH mixing matrices are found to be different as is expected given the asymmetrical form of the mass matrices.

We studied the possibility of differentiating between the case of symmetrical and asymmetrical quark mass matrices from flavor changing top decays, $t \rightarrow Z + \text{jets}$. We found the dominant mode of decay is that with a final state charm jet. The total branching ratio is calculated to be ~ 3 to 5×10^{-6} in the symmetrical case and $\sim 9 \times 10^{-6}$ to 2×10^{-5} in the asymmetrical case. The signal is within reach of the LHC which has been estimated to be 6.5×10^{-5} for a 5σ signal at 100 fb^{-1} [25]. However, the difference between the two cases may be difficult to discern.

We have also investigated the decay $t_R \rightarrow b_R W$ as a large number of top quarks are expected to be produced at the LHC. We found a branching ratio at the level of $\mathcal{O}(10^{-5})$ is possible. Although the signal is not negligible,

given the huge SM background, its detection is still a very challenging task, and a careful feasibility study is needed. This is beyond the scope of the present paper.

ACKNOWLEDGMENTS

W.F.C. is grateful to the TRIUMF Theory group for their hospitality when part of this work was completed. The research of J.N.N. and J.M.S.W. is partially supported by the Natural Science and Engineering Council of Canada. The work of W.F.C. is supported by the Taiwan NSC under Grant No. 96-2112-M-007-020-MY3.

Note added:—After the completion of this work, we became aware of Ref. [28] which finds that flavor bounds from the $\Delta F = 2$ processes in the meson sector, in particular that from ϵ_K , might require the KK mass scale to be generically $\mathcal{O}(10)$ TeV in the MCRS model. We will show in an ensuing publication [29] that parameter space generically exists where KK mass scale of a few TeV is still consistent with all the flavor constraints from meson mixings, and that our conclusions with regard to the top decay in this work continue to hold.

APPENDIX A: THE HERMITIAN MASS MATRIX ANSATZ

In this Appendix we show that generically, the Fritzsche-type ansatz cannot be accommodated in the RS framework without requiring a hierarchy in the 5D Yukawa couplings. We consider below a general Hermitian mass matrix ansatz for which the Fritzsche-type ansatz is a special case of.

1. General analytical structure

The Hermitian mass matrix ansatz takes the form

$$M_f = P_f^\dagger \hat{M}_f P_f, \quad f = u, d, \quad (\text{A1})$$

where $P_f = \text{diag}\{1, e^{i\phi_{c_f}}, e^{i(\phi_{b_f} + \phi_{c_f})}\}$ is a diagonal pure phase matrix, and

$$\hat{M}_f = \begin{pmatrix} U_f & |C_f| & V_f \\ |C_f| & D_f & |B_f| \\ V_f^* & |B_f| & A_f \end{pmatrix}, \quad V_f = |V_f| e^{i\omega_f}, \quad (\text{A2})$$

$$\omega_f = \phi_{b_f} + \phi_{c_f} - \phi_{v_f},$$

with $\phi_X \equiv \arg(X)$ and $A_f, D_f, U_f, |X|, \phi_X \in \mathbb{R}$. Note that the Fritzsche-type ansatz with four texture zeros [15] is recovered when $U_f = V_f = 0$ (the six-zero texture case [14] has $D_f = 0$ also). For simplicity, we take $\omega_f \in \{0, \pi\}$ below so that $V_f = \pm |V_f|$.⁶ We will ignore the fermion label below for convenience.

The matrix \hat{M} can be diagonalized via an orthogonal transformation

$$O^T \hat{M} O = \begin{pmatrix} \lambda_1 & 0 & 0 \\ 0 & \lambda_2 & 0 \\ 0 & 0 & \lambda_3 \end{pmatrix}, \quad |\lambda_1| < |\lambda_2| < |\lambda_3|. \quad (\text{A3})$$

The eigenvalues $|\lambda_i|$, $i = 1, 2, 3$, can be either positive or negative. To reproduce the observed mass spectrum, we set $|\lambda_i| = m_i$. From the observed quark mass hierarchy, it is expected in general that $|A|$ be the largest entries in \hat{M} , and $|A| \lesssim |\lambda_3|$. Without loss of generality, we take A and λ_3 to be positive.

By applying the Cayley-Hamilton theorem, three independent relations between the six parameters of \hat{M} to its three eigenvalues can be deduced:

$$\begin{aligned} S_1 - A - D - U &= 0, \\ S_2 + |B|^2 + |C|^2 + V^2 - AD - (A + D)U &= 0, \\ S_3 + A|C|^2 + DV^2 + U|B|^2 - ADU - 2|B||C|V &= 0, \end{aligned} \quad (\text{A4})$$

where

$$S_1 = \sum_i \lambda_i, \quad S_2 = \sum_{i < j} \lambda_i \lambda_j, \quad S_3 = \prod_i \lambda_i.$$

Choosing A, U, V to be the free parameters, Eq. (A4) can be solved for $|B|, |C|$, and D :

$$\begin{aligned} D &= S_1 - A - U, \\ |B| &= \frac{VY + Z}{\sqrt{(A - U)X - 2V(VY + Z)}}, \\ |C| &= \sqrt{\frac{(A - U)X - 2V(VY - Z)}{(A - U)^2 + 4V^2}}, \end{aligned} \quad (\text{A5})$$

where

$$\begin{aligned} X &= U^3 + (A + 2U)V^2 - (U^2 + V^2)S_1 + US_2 - S_3, \\ Y &= A^2 + V^2 + (A + U)(U - S_1) + S_2, \\ Z &= \sqrt{V^2 Y^2 + (U - A)XY - X^2}. \end{aligned} \quad (\text{A6})$$

If $|U|, |V| \ll |\lambda_1| \ll |A|$ so that Eq. (A1) is a perturbation of the Fritzsche four-zero texture ansatz, $|B|$ and $|C|$ can be expanded as

$$\begin{aligned} |B| &= \pm \sqrt{\frac{-1}{A} \prod_i (A - \lambda_i)} \left[1 + \frac{\epsilon_U}{2} \mp \epsilon_V R + \mathcal{O}(\epsilon_U^2, \epsilon_V^2) \right] \\ &\quad + \frac{VA^{3/2}}{\sqrt{-S_3}} \left(1 - \frac{S_1}{A} + \frac{S_2}{A^2} \right) \left[1 + \frac{US_2}{2S_3} + \frac{\epsilon_U}{2} \mp \epsilon_V R(A) \right. \\ &\quad \left. + \mathcal{O}(\epsilon_U^2, \epsilon_V^2) \right], \\ |C| &= \sqrt{\frac{-S_3}{A}} \left[1 - \frac{US_2}{2S_3} + \frac{\epsilon_U}{2} \mp \epsilon_V R + \mathcal{O}(\epsilon_U^2, \epsilon_V^2) \right], \end{aligned} \quad (\text{A7})$$

⁶Such case has been considered in Ref. [26], and was shown to be consistent with the current experimental CKM data.

where

$$\epsilon_U = \frac{U}{A}, \quad \epsilon_V = \frac{V}{A}, \quad R = \sqrt{\frac{1}{S_3} \prod_i (A - \lambda_i)}. \quad (\text{A8})$$

Given that we have taken $A < \lambda_3$ and $A, \lambda_3 > 0$, it is required that $S_3 < 0$ (or $\lambda_1 \lambda_2 < 0$) for $|B|$ and $|C|$ to be real. This is consistent with the expectation from the considerations of Ref. [15]. In the limit $U, V \rightarrow 0$, the exact Fritzsch four-zero texture ansatz is recovered.

With \hat{M} determined by the three free parameters which we chose to be A, U , and V , so are its eigenvectors. For each eigenvalue λ_i , its associated eigenvector takes the form

$$\mathbf{v}_i = \begin{pmatrix} |C|(A - \lambda_i) - |B|V \\ V^2 - (A - \lambda_i)(U - \lambda_i) \\ |B|(U - \lambda_i) - |C|V \end{pmatrix}. \quad (\text{A9})$$

The orthogonal matrix O is then given by

$$O = \begin{pmatrix} | & | & | \\ \bar{\mathbf{v}}_1 & \bar{\mathbf{v}}_2 & \bar{\mathbf{v}}_3 \\ | & | & | \end{pmatrix}, \quad \bar{\mathbf{v}}_i \equiv \frac{\mathbf{v}_i}{\|\mathbf{v}_i\|}, \quad i = 1, 2, 3, \quad (\text{A10})$$

and the quark mixing matrix by $V_{\text{mix}} \equiv O_u^T (P_u P_d^\dagger) O_d$.

2. Matching to the RS mass matrix

To reproduce the Hermitian mass matrix ansatz (A1) by the RS mass matrix (25), we match them and solve for the parameters determining the RS mass matrix. For the purpose of checking if hierarchy arises in the 5D Yukawa couplings from the matching, we may start matching in either the up or the down sector. For simplicity, the fermion species label is ignored below.

There are a total of 24 parameters in M^{RS} to be determined: six fermion wave function values, $F_L(c_i^L)$ and $F_R(c_i^R)$, nine Yukawa magnitudes, ρ_{ij} , and nine Yukawa phases, ϕ_{ij} , where $i, j = 1, 2, 3$. Matching results in nine conditions for both the magnitudes and the phases. Thus all the Yukawa phases are determined by $\phi_{B,C}$, while six magnitudes are left as free independent parameters. These we chose to be $F_L(c_3^L)$ and $F_R(c_3^R)$, which are constrained by EWPT, and $\rho_{11}, \rho_{21}, \rho_{31}, \rho_{32}$. The determined parameters are then the five Yukawa magnitudes:

$$\begin{aligned} \rho_{13} &= \frac{kL}{F_L(c_3^L)F_R(c_3^R)} \frac{V^2}{v_W U} \frac{\rho_{11}}{\rho_{31}}, \\ \rho_{23} &= \frac{kL}{F_L(c_3^L)F_R(c_3^R)} \frac{V|B|}{v_W |C|} \frac{\rho_{21}}{\rho_{31}}, \\ \rho_{33} &= \frac{kL}{F_L(c_3^L)F_R(c_3^R)} \frac{A}{v_W}, \\ \rho_{12} &= \frac{|C|V}{|B|U} \frac{\rho_{11}\rho_{32}}{\rho_{31}}, \\ \rho_{22} &= \frac{DV}{|B||C|} \frac{\rho_{21}\rho_{32}}{\rho_{31}}, \end{aligned} \quad (\text{A11})$$

the nine Yukawa phases:

$$(\phi_{ij}) = \begin{pmatrix} 0 & \phi_C & \phi_B + \phi_C \\ -\phi_C & 0 & \phi_B \\ -\phi_B - \phi_C & -\phi_B & 0 \end{pmatrix}, \quad (\text{A12})$$

and the four fermion wave function values:

$$\begin{aligned} F_L(c_1^L) &= F_L(c_3^L) \frac{U}{V} \frac{\rho_{31}}{\rho_{11}}, & F_L(c_2^L) &= F_L(c_3^L) \frac{|C|}{V} \frac{\rho_{31}}{\rho_{21}}, \\ F_R(c_1^R) &= \frac{V}{v_W} \frac{kL}{F_L(c_3^L)\rho_{31}}, & F_R(c_2^R) &= \frac{|B|}{v_W} \frac{kL}{F_L(c_3^L)\rho_{32}}. \end{aligned} \quad (\text{A13})$$

Note that there are only three independent Yukawa phases because the mass matrix ansatz is Hermitian. Note also that since fermion wave functions are always positive, V and thus U have to be positive implying that $\omega = 0$.

From Eq. (A11), in order for the Yukawa couplings to be of the same order, it is required that $\rho_{11} \sim \rho_{21} \sim \rho_{31} \sim \rho_{32} \sim \rho_{33}$, and

$$\begin{aligned} \frac{|C|V}{|B|U} \sim 1, & \quad \frac{DV}{|B||C|} \sim 1, & \quad \frac{V^2}{UA} \sim 1 \\ \Rightarrow \frac{V}{U} \sim \frac{A}{V} \sim \frac{|B|}{|C|}. \end{aligned} \quad (\text{A14})$$

For generic sets of parameters we find $|B_u|/|C_u| \sim \mathcal{O}(10^3)$ and $|B_d|/|C_d| \sim \mathcal{O}(50)$. However, parameter sets that reproduce all entries of the CKM matrix and also the Jarlskog invariant to within two standard error can only be found if $V_u \sim U_u$ and $V_d \sim 10U_d$. Thus hierarchy in the 5D Yukawa couplings cannot be avoided if the Hermitian mass matrix ansatz (A1) is to be accommodated in the RS framework.

APPENDIX B: RS MATCHING OF THE SYMMETRIC ANSATZ

In this Appendix, we give analytical expressions for the parameters determined from matching the RS mass matrix (25) to the mass matrix ansatz (26). Starting with the up sector, the determined parameters are the five up-type Yukawa magnitudes:

$$\begin{aligned}
\rho_{13}^u &= \frac{kL}{F_L(c_{Q_3})F_R(c_{U_3})} \frac{C_u^2}{v_W \xi_u} \frac{\rho_{11}^u}{\rho_{31}^u}, \\
\rho_{23}^u &= \frac{kL}{F_L(c_{Q_3})F_R(c_{U_3})} \frac{B_u}{v_W} \frac{\rho_{21}^u}{\rho_{31}^u}, \\
\rho_{33}^u &= \frac{kL}{F_L(c_{Q_3})F_R(c_{U_3})} \frac{A_u}{v_W}, \\
\rho_{12}^u &= \frac{C_u^2}{B_u \xi_u} \frac{\rho_{11}^u \rho_{32}^u}{\rho_{31}^u}, \\
\rho_{22}^u &= \frac{A_u}{B_u} \frac{\rho_{21}^u \rho_{32}^u}{\rho_{31}^u},
\end{aligned} \tag{B1}$$

the nine up-type Yukawa phases:

$$(\phi_{ij}^u) = \begin{cases} -2\delta_i^u, & i = j \\ -\delta_i^u - \delta_j^u, & i \neq j, \end{cases} \tag{B2}$$

and the four fermion wave function values:

$$\begin{aligned}
F_L(c_{Q_1}) &= F_L(c_{Q_3}) \frac{\xi_u}{C_u} \frac{\rho_{31}^u}{\rho_{11}^u}, \\
F_L(c_{Q_2}) &= F_L(c_{Q_3}) \frac{\rho_{31}^u}{\rho_{21}^u}, \\
F_R(c_{U_1}) &= \frac{kL}{F_L(c_{Q_3})} \frac{C_u}{v_W} \frac{1}{\rho_{31}^u}, \\
F_R(c_{U_2}) &= \frac{kL}{F_L(c_{Q_3})} \frac{B_u}{v_W} \frac{1}{\rho_{32}^u}.
\end{aligned} \tag{B3}$$

Next is the down sector. Given the information on the up sector, the determined parameters are the six down-type Yukawa magnitudes:

$$\begin{aligned}
\rho_{11}^d &= \frac{F_L(c_{Q_3})}{F_L(c_{Q_1})} \frac{\xi_d}{C_d} \rho_{31}^d = \frac{C_u}{\xi_u} \frac{\xi_d}{C_d} \frac{\rho_{11}^u}{\rho_{31}^u} \rho_{31}^d, \\
\rho_{21}^d &= \frac{F_L(c_{Q_3})}{F_L(c_{Q_2})} \rho_{32}^d = \frac{\rho_{21}^u}{\rho_{31}^u} \rho_{31}^d, \\
\rho_{12}^d &= \frac{F_L(c_{Q_3})}{F_L(c_{Q_1})} \frac{C_d}{|B_d|} \rho_{32}^d = \frac{C_u}{\xi_u} \frac{C_d}{|B_d|} \frac{\rho_{11}^u}{\rho_{31}^u} \rho_{32}^d, \\
\rho_{22}^d &= \frac{F_L(c_{Q_3})}{F_L(c_{Q_2})} \frac{A_d}{|B_d|} \rho_{32}^d = \frac{A_d}{|B_d|} \frac{\rho_{21}^u}{\rho_{31}^u} \rho_{32}^d, \\
\rho_{13}^d &= \frac{F_L(c_{Q_3})}{F_L(c_{Q_1})} \frac{C_d}{A_d} \rho_{33}^d = \frac{C_u}{\xi_u} \frac{C_d}{A_d} \frac{\rho_{11}^u}{\rho_{31}^u} \rho_{33}^d, \\
\rho_{23}^d &= \frac{F_L(c_{Q_3})}{F_L(c_{Q_2})} \frac{|B_d|}{A_d} \rho_{33}^d = \frac{|B_d|}{A_d} \frac{\rho_{21}^u}{\rho_{31}^u} \rho_{33}^d,
\end{aligned} \tag{B4}$$

the nine down-type Yukawa phases:

$$(\phi_{ij}^d) = \begin{cases} -2\delta_i^d, & i = j \\ -\delta_i^d - \delta_j^d + \pi(\delta_{2i}\delta_{3j} + \delta_{2j}\delta_{3i}), & i \neq j, \end{cases} \tag{B5}$$

and the three fermion wave function values:

$$\begin{aligned}
F_R(c_{D_1}) &= \frac{C_d}{v_W} \frac{kL}{F_L(c_{Q_3})} \frac{1}{\rho_{31}^d}, \\
F_R(c_{D_2}) &= \frac{|B_d|}{v_W} \frac{kL}{F_L(c_{Q_3})} \frac{1}{\rho_{32}^d}, \\
F_R(c_{D_3}) &= \frac{A_d}{v_W} \frac{kL}{F_L(c_{Q_3})} \frac{1}{\rho_{33}^d}.
\end{aligned} \tag{B6}$$

Note that there are only six independent up-type Yukawa phases and six for the down-type Yukawa phases since the mass matrix ansatz is symmetric. With the texture phases $\delta_{1,2,3}^f$ determined by fitting the CKM data, there are three more relations, i.e. $\delta_1^d = \delta_1^u = 0$ and $\delta_{2,3}^d = \delta_{2,3}^u - \delta_{2,3}^d$, which further reduce the number of independent Yukawa phases from a total of 12 down to nine.

In order to be consistent with EWPT ($\delta g_{Zb_L \bar{b}_L} / g_{Zb_L \bar{b}_L} \lesssim 0.01^7$) and to avoid too large a correction to the Peskin-Takeuchi S and T parameters, it is required that $0.25 < c_{Q_3} < 0.4$, $c_{U_3} < 0.2$, so that $m_{\text{gauge}}^{(1)} \lesssim 4$ TeV [11]. To have the theory weakly coupled for at least the first two KK modes, $|\lambda_5| < 4$ is required also [20]. It follows that $2.70 < F_L(c_{Q_3}) < 4.27$, $F_R(c_{U_3}) < 7.15$, and $\rho_{ij}^{u,d} < 4$, which when combined with Eqs. (B1), (B4), (37), and (39) imply

$$4.06 < F_L(c_{Q_3})F_R(c_{U_3}) < 30.57, \quad 0.53 < \rho_{33}^u < 4, \tag{B7}$$

and

$$\begin{aligned}
\frac{\rho_{11}^u}{\rho_{31}^u} &< 0.14 F_L(c_{Q_3}) F_R(c_{U_3}), \\
\frac{\rho_{21}^u}{\rho_{31}^u} &< 0.25 F_L(c_{Q_3}) F_R(c_{U_3}),
\end{aligned} \tag{B8}$$

⁷The bound we adopted here is that from the PDG. Studies of similar model but differing details where a complete electroweak analysis was carried out have produced a more stringent bound, e.g. $\lesssim 0.0025$ [27]. Such complete EWPT analysis, however, is beyond the scope of the present work.

$$\begin{aligned}
\frac{\rho_{31}^u}{\rho_{31}^d} \rho_{32}^u &< 2.19, & \frac{\rho_{31}^u}{\rho_{31}^d} \rho_{31}^d &< 1.52, \\
\frac{\rho_{31}^u}{\rho_{31}^d} \rho_{32}^d &< 1.92, & \frac{\rho_{31}^u}{\rho_{31}^d} \rho_{33}^d &< 1.99, \\
\frac{\rho_{21}^u}{\rho_{31}^u} \rho_{32}^u &< 3.97, & \frac{\rho_{21}^u}{\rho_{31}^u} \rho_{31}^d &< 4, \\
\frac{\rho_{21}^u}{\rho_{31}^u} \rho_{32}^d &< 3.86, & \frac{\rho_{21}^u}{\rho_{31}^u} \rho_{33}^d &< 4.15.
\end{aligned}
\tag{B9}$$

Observe from Eq. (B3) that the second generation $SU(2)_L$ doublet, Q_2 , is localized towards the UV (IR) brane if ρ_{31}^u/ρ_{21}^u is less (greater) than $F_L(0.5 + \epsilon)/F_L(c_{Q_3})$ ($F_L(0.5 - \epsilon)/F_L(c_{Q_3})$). Note that $F_L(0.5 \pm \epsilon) \approx 1 \mp \epsilon k r_c \pi$ for $\epsilon \ll 1/(2kr_c\pi)$. We plot in Fig. 6 the critical value of ρ_{31}^u/ρ_{21}^u below (above) which Q_2 is localized towards the UV (IR) brane. The same logic shows that the first generation $SU(2)_L$ doublet, Q_1 , is generically localized towards the UV brane because of the suppression factor $\xi_u/C_u \sim 10^{-2}$ (even if $\rho_{31}^u/\rho_{11}^u \geq 1$).

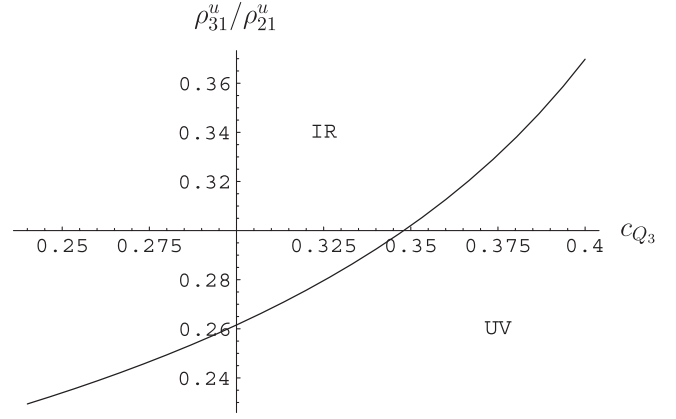


FIG. 6. The critical value of ρ_{31}^u/ρ_{21}^u as a function of c_{Q_3} in the range allowed by EWPT. For values of ρ_{31}^u/ρ_{21}^u in the “UV” (“IR”) region, c_{Q_2} is greater (less) than 0.5.

-
- [1] N. Arkani-Hamed, S. Dimopoulos, and G. R. Dvali, Phys. Lett. B **429**, 263 (1998); I. Antoniadis, N. Arkani-Hamed, S. Dimopoulos, and G. R. Dvali, Phys. Lett. B **436**, 257 (1998).
- [2] L. Randall and R. Sundrum, Phys. Rev. Lett. **83**, 3370 (1999).
- [3] N. Arkani-Hamed and M. Schmaltz, Phys. Rev. D **61**, 033005 (2000).
- [4] See e.g. G. R. Dvali and M. A. Shifman, Phys. Lett. B **475**, 295 (2000); D. E. Kaplan and T. M. P. Tait, J. High Energy Phys. 06 (2000) 020; 11 (2001) 051; M. V. Libanov and S. V. Troitsky, Nucl. Phys. **B599**, 319 (2001); J. M. Frere, M. V. Libanov, and S. V. Troitsky, Phys. Lett. B **512**, 169 (2001).
- [5] Y. Grossman and M. Neubert, Phys. Lett. B **474**, 361 (2000).
- [6] T. Gherghetta and A. Pomarol, Nucl. Phys. **B586**, 141 (2000); S. J. Huber and Q. Shafi, Phys. Lett. B **498**, 256 (2001).
- [7] E. A. Mirabelli and M. Schmaltz, Phys. Rev. D **61**, 113011 (2000); W. F. Chang and J. N. Ng, J. High Energy Phys. 12 (2002) 077.
- [8] S. J. Huber, Nucl. Phys. **B666**, 269 (2003).
- [9] S. Chang, C. S. Kim, and M. Yamaguchi, Phys. Rev. D **73**, 033002 (2006).
- [10] G. Moreau and J. I. Silva-Marcos, J. High Energy Phys. 01 (2006) 048; 03 (2006) 090.
- [11] K. Agashe, A. Delgado, M. J. May, and R. Sundrum, J. High Energy Phys. 08 (2003) 050.
- [12] A. Pomarol, Phys. Lett. B **486**, 153 (2000).
- [13] Z. Z. Xing, H. Zhang, and S. Zhou, Phys. Rev. D **77**, 113016 (2008).
- [14] H. Fritzsch, Phys. Lett. **73B**, 317 (1978); Nucl. Phys. **B155**, 189 (1979).
- [15] H. Fritzsch and Z. Z. Xing, Phys. Lett. B **555**, 63 (2003).
- [16] Y. Koide, H. Nishiura, K. Matsuda, T. Kikuchi, and T. Fukuyama, Phys. Rev. D **66**, 093006 (2002).
- [17] K. Matsuda and H. Nishiura, Phys. Rev. D **69**, 053005 (2004).
- [18] A. Delgado, A. Pomarol, and M. Quiro, J. High Energy Phys. 01 (2000) 030; W. F. Chang, I.-L. Ho, and J. N. Ng, Phys. Rev. D **66**, 076004 (2002); S. Khalil and R. Mohapatra, Nucl. Phys. **B695**, 313 (2004).
- [19] See e.g. R. Kitano, Phys. Lett. B **481**, 39 (2000); G. Burdman, Phys. Rev. D **66**, 076003 (2002); C. S. Kim, J. D. Kim, and J. H. Song, Phys. Rev. D **67**, 015001 (2003).
- [20] K. Agashe, G. Perez, and A. Soni, Phys. Rev. D **71**, 016002 (2005).
- [21] M. S. Carena, A. Delgado, E. Ponton, T. M. P. Tait, and C. E. M. Wagner, Phys. Rev. D **68**, 035010 (2003).
- [22] M. S. Carena, E. Ponton, J. Santiago, and C. E. M. Wagner, Nucl. Phys. **B759**, 202 (2006).
- [23] J. L. Díaz-Cruz, R. Martínez, M. A. Pérez, and A. Rosado, Phys. Rev. D **41**, 891 (1990); G. Eilam, J. L. Hewett, and A. Soni, Phys. Rev. D **44**, 1473 (1991); B. Mele, S. Petrarca, and A. Soddu, Phys. Lett. B **435**, 401 (1998).
- [24] K. Agashe, G. Perez, and A. Soni, Phys. Rev. D **75**, 015002 (2007).
- [25] J. Carvalho, N. Castro, A. Onofre, and F. Veloso, ATL-PHYS-PUB-2005-026, ATL-COM-PHYS-2005-059 (Atlas Internal Notes).
- [26] Z. Q. Guo and B. Q. Ma, Phys. Lett. B **647**, 436 (2007).
- [27] K. Agashe and R. Contino, Nucl. Phys. **B742**, 59 (2006).
- [28] C. Csaki, A. Falkowski, and A. Weiler, J. High Energy Phys. 09 (2008) 008.
- [29] W. F. Chang, J. N. Ng, and J. M. S. Wu, arXiv:0809.1390.